Support Information

Compositional Doping and Structure Insights for High-Performance Aqueous Zn-Ion Batteries

Jianxin Yang,†[a] Yuchen Jiang,†[a] Tao Wang,[a] Shuai Tong,[a] Yang Wang,[a] Dianwu Kang,[a] Shutong Lu,[a] Mengqi Zhang,[a] Min Jia*[a] and Xiaoyu Zhang*[a]

a. School of Material Science and Engineering, Jiangsu University, Zhenjiang, 212013, China. E-mail: mjia@ujs.edu.cn; x.zhang@ujs.edu.cn.

† These authors contributed equally to this work.

Synthesis of Mg-MnO

MnO was synthesized using a co-precipitation method followed by high-temperature calcination. A mixture of 200 mL of $MnSO_4 \cdot H_2O$ solution and 100 mL of Na_2CO_3 solution (with a molar ratio of 2:1) was slowly added to a mixture of ethanol and water, stirred continuously for 2 hours, then left to stand for 1 hour before centrifugation. The resulting manganese carbonate precursor was dried overnight in a 70°C oven. Subsequently, the carbonate was calcined in a tube furnace filled with argon at 600°C for 2 hours to obtain MnO. To synthesize Mg-doped MnO with varying magnesium content, different amounts of $Mg(NO_3)_2 \cdot 6H_2O$ were added to the manganese sulfate solution, while keeping all other conditions constant.[1]

Assembled coin AZIBs and electrochemical measurement

The electrochemical evaluation was carried out by assembling into a CR2032-type coin cell. The cathode consisted of Mg-MnO, acetylene black and polytetrafluoroethylene (PVDF) were mixed by a mass ratio of 7:2:1 and suitable N-methyl pyrrolidone (NMP) was added to the mixed powder. Then put the mixture on the the magnetic mixer,stirring for 2 hours to obtain the uniform slurry before being coated on a stainless steel wire and dried at 80 ℃ for whole night by vacuum. Then, the electrodes were cut into circular pole pieces with a diameter of 12 mm. Zinc foils(16 mm) and glass fiber membranes(16 mm) (Whatman, GF/A) were used as the anode and separators. The electrolyte used was an aqueous solution of 2 M $ZnSO_4$ and 0.2 M $MnSO_4$.

The cycle performance and rate performance were measured on a battery test system (LAND System, Wuhan). Cyclic voltammetry (CV) was performed on an electrochemical workstation (CHI760E, Shanghai).

Materials characterization

X-ray diffraction (XRD) patterns were investigated on a Bruker D8 X-ray diffractometer with Cu K radiation.The morphology was conducted by scanning electron microscopy (SEM,ZEISS GeminiSEM 300) and the transmission electron microscopy (TEM, FEI Tecnai F20).The chemical composition and element valence of Mg-MnO were measured by X-ray photoelectron spectroscopy (XPS, Thermo Scientific K-Alpha).

GITT Calculations

Galvanostatic intermittence titration technique (GITT) technique was used to calculate the Zn^{2+} diffusivity coefficient reflecting the kinetic behavior of Mg-MnO and the Zn^{2+} diffusivity coefficient was calculated based on equation:

$$D=\frac{4L^2}{\pi\tau}\left(\frac{\Delta Es}{\Delta Et}\right)^2$$

Where τ is the relaxation time (s), L is diffusion length (cm) of Zn^{2+} which is equal to thickness of electrode, and ΔEs is the steady-state potential change (V) by the current pulse. ΔEt is the potential change (V) during the constant current pulse after eliminating the iR drop. Current pulse of 100 mA g^{-1} was applied for 20 minutes while the followed relaxation time is 90 minutes.

Computational details

All the calculations are performed in the framework of the density functional theory with the projector augmented plane-wave method, as implemented in the Vienna ab initio simulation package.[2] The generalized gradient approximation proposed by Perdew-Burke-Ernzerhof (PBE) is selected for the exchange-correlation potential.[3] The cut-off energy for plane wave is set to 480 eV. The energy criterion is set to 10^{-4} eV in the iterative solution of the Kohn-Sham equation. All the structures are relaxed until the residual forces on the atoms have declined to less than 0.05 eV/Å. To avoid interlaminar interactions, a vacuum spacing of 20 Å is applied perpendicular to the slab.

Table S1. Comparison of design values of Mg:Mn and actual values measured by ICP.

Designed Mg:Mn	ICP determined Mg:Mn
3:100	3.42779:100
4:100	4.35756:100
5:100	4.93704:100
6:100	5.94055:100

Table S2. Crystallographic data obtained from Rietveld refinements of the XRD patterns of the Mg-MnO (5%).

Lattice parameters(Å)	a=b=c=4.401029
Volume(Å3)	85.244
Error factor	wRp=4.82% Rp=3.15%
Mg/Mn-O(Å)	2.20051(2)
Mn-Mg(Å)	3.11200(2)

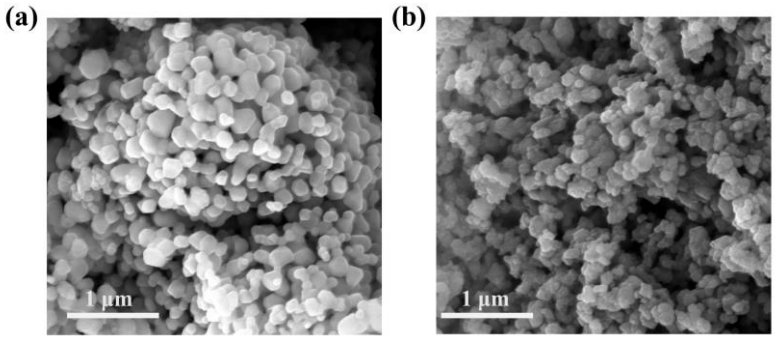

Fig. S1. SEM images of (a) pure MnO and (b) Mg-MnO(5%).

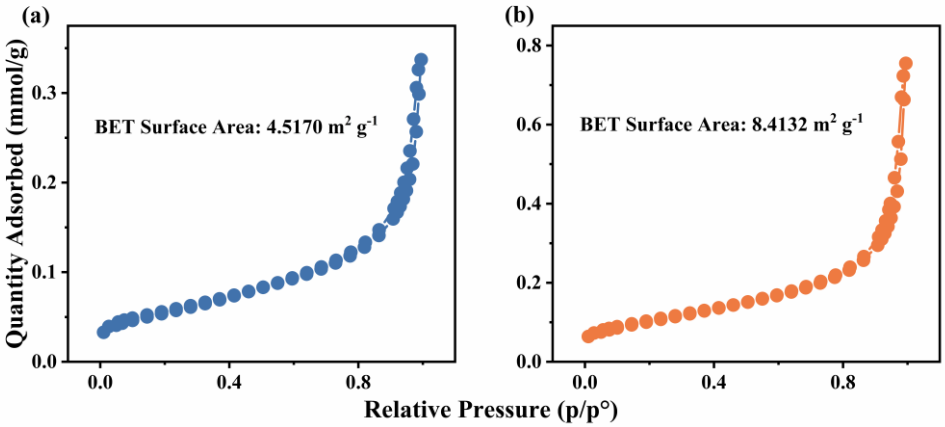

Fig. S2. N_2 adsorption/desorption isotherm of (a) pure MnO and (b) Mg-MnO(5%).

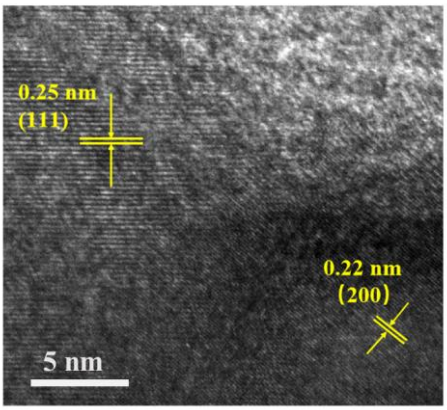

Fig. S3.TEM images of Mg-MnO(5%).

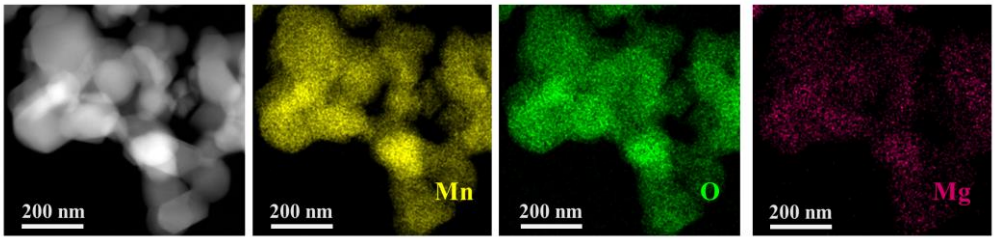

Fig. S4.EDX results of Mg-MnO(5%).

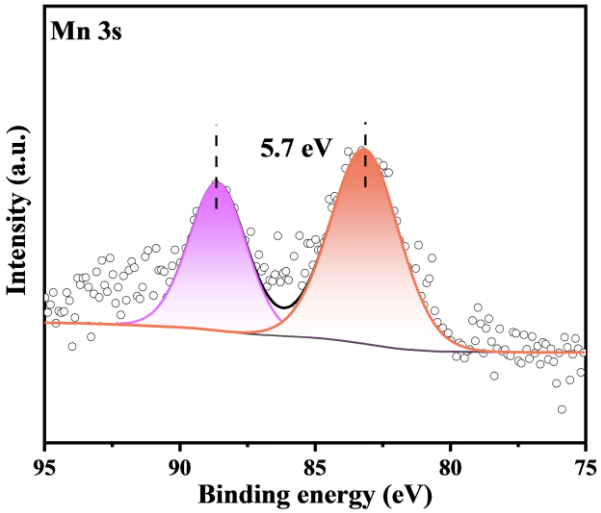

Fig. S5. XPS spectra of Mg-MnO(5%) of Mn 3s.

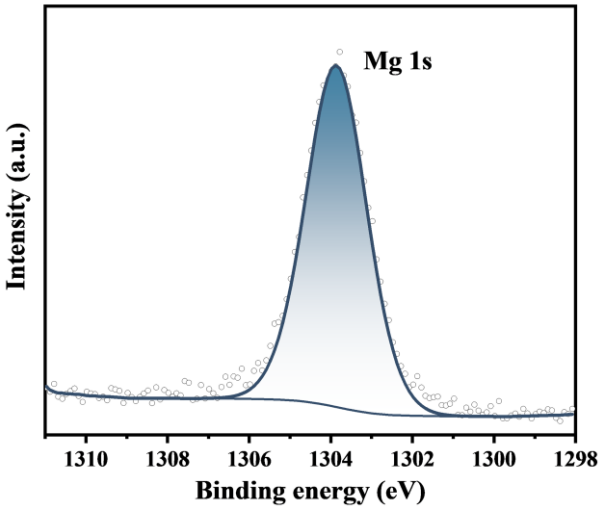

Fig. S6. XPS spectra of Mg-MnO(5%) of Mg 1s.

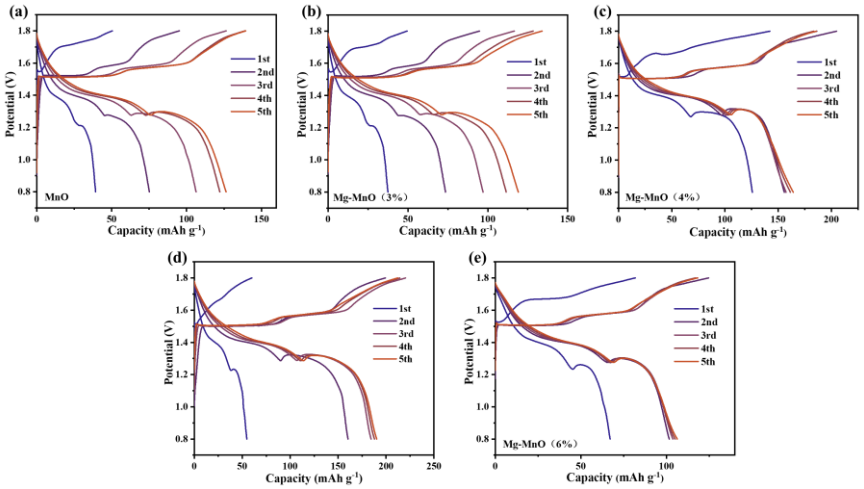

Fig. S7. The first five charge/discharge curves of the (a) pure MnO, (b) Mg-MnO(3%), (c) Mg-MnO(4%), (d) Mg-MnO(5%) and (e) Mg-MnO(6%) at 0.1 A g^{-1}.

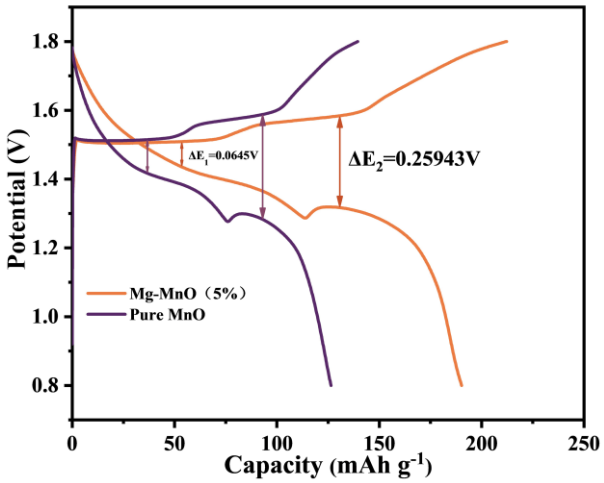

Fig. S8. The comparison of potential difference between MnO and Mg-MnO(5%).

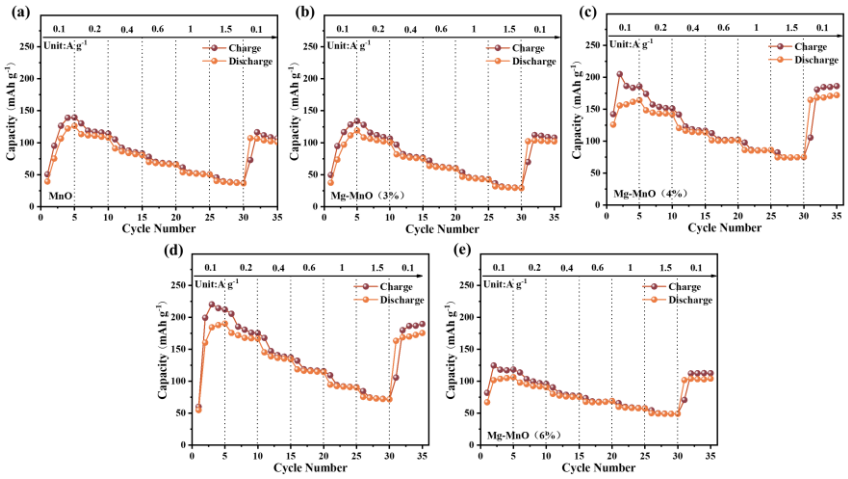

Fig. S9. The rate capabilities of the (a) pure MnO, (b) Mg-MnO(3%), (c) Mg-MnO(4%), (d) Mg-MnO(5%) and (e) Mg-MnO(6%) at 0.1 A g^{-1}.

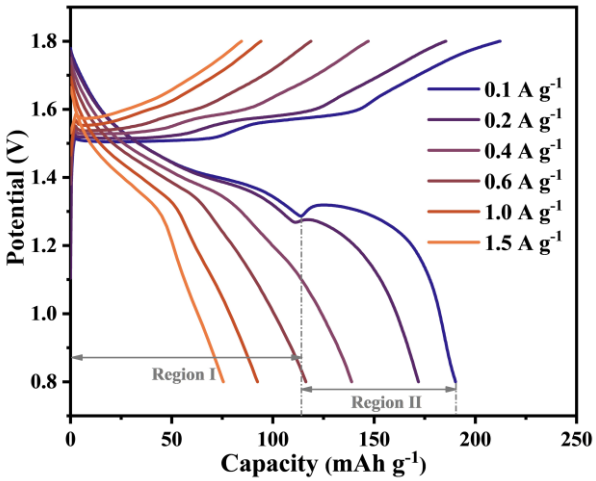

Fig. S10. Charge/discharge curves of Mg-MnO(5%) at different current densities.

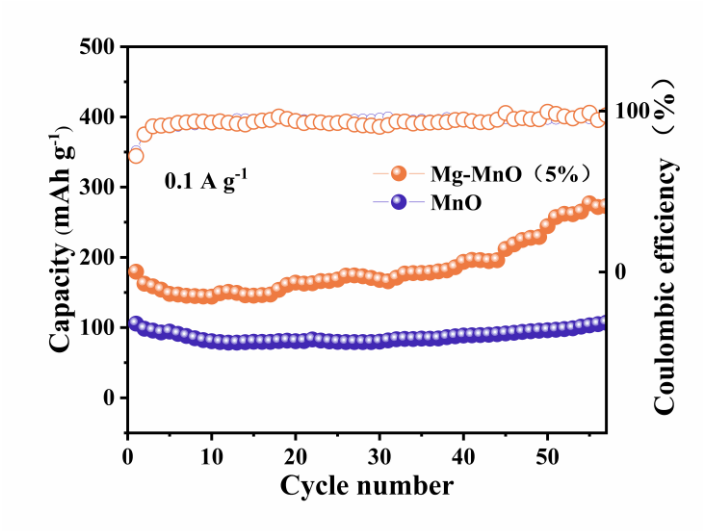

Fig. S11. Cycling performance at a current density of 0.1 A g^{-1} for the MnO and Mg-MnO(5%).

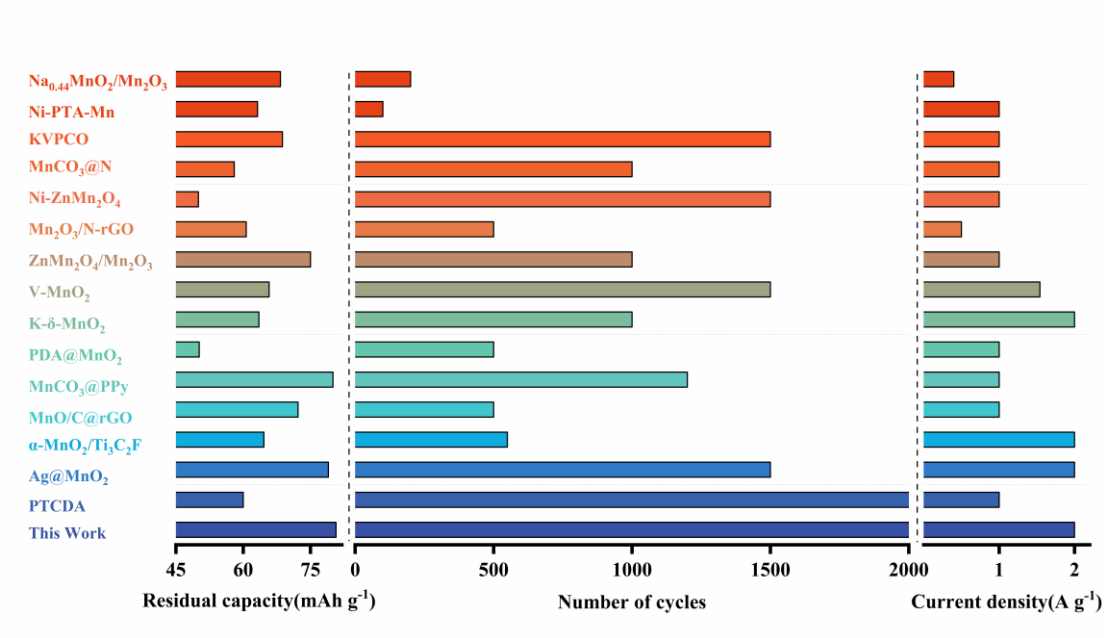

Fig. S12. Comparison of residual capacity after long-term cycling between this study and existing literature.[4-18]

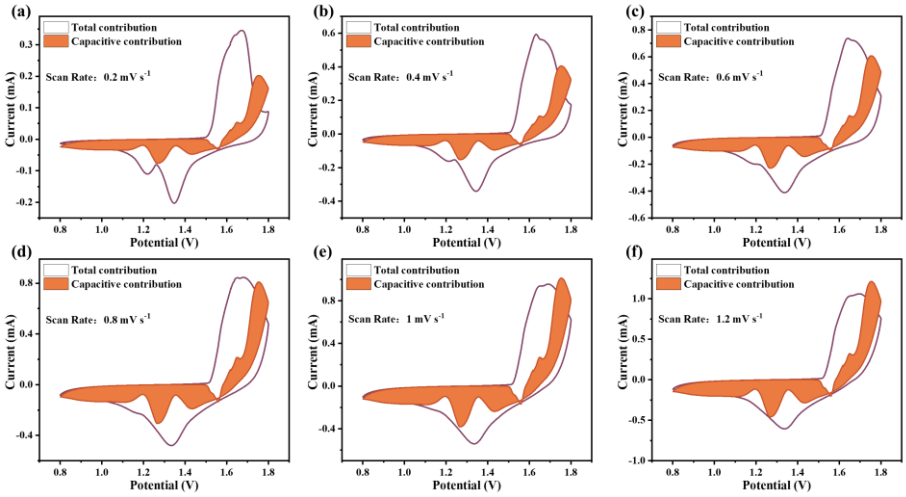

Fig. S13. Contribution ratios of the capacitive and diffusion-controlled capacities for Mg-MnO(5%) at (a) 0.2 mV s^{-1}, (b) 0.4 mV s^{-1}, (c) 0.6 mV s^{-1}, (d) 0.8 mV s^{-1}, (e) 1 mV $s^{-1}$and (f) 1.2 mV s^{-1}.

Table S3. Comparison of Mg:Mn ratios in the initial state and after the first charge cycle measured by ICP.

State	Mg: Mn
Pristine	4.93704:100
1 charge	14.9507:100

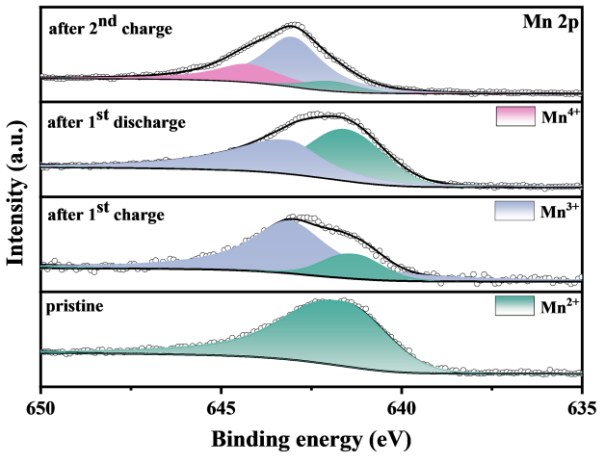

Fig. S14. Ex-situ XPS spectra of Mg-MnO(5%) of Mn 2p.

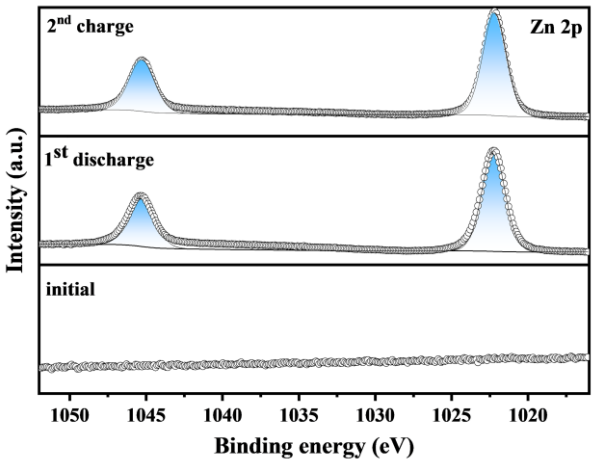

Fig. S15. Ex-situ XPS spectra of Mg-MnO(5%) of Zn 2p.

Table. S4. Comparison study of the integrated DOS plot from -1.0 eV to 1.0 eV for MnO and Mg-MnO.

DOS	MnO	Mg-MnO
TDOS	100.0%	100.0%
Mn 3d	68.21%	77.28%
O 2p	17.34%	10.03%

Reference:

1. B. He, J. Huang, P. Ji, T. K. A. Hoang, M. Han, L. Li, L. Zhang, Z. Gao, J. Ma, J. Zhi and P. Chen, *Journal of Power Sources*, 2023, **554**, 232353.
2. G. Kresse and D. Joubert, *Physical Review B*, 1999, **59**, 1758-1775.
3. K. B. John P. Perdew, Matthias Ernzerhof, *PHYSICAL REVIEW LETTERS*, 1996, **77**, 3865-3868.
4. F. Yu, Y. Wang, Y. Liu, H.-Y. Hui, F.-X. Wang, J.-F. Li and Q. Wang, *Rare Metals*, 2022, **41**, 2230-2236.
5. Y. Wang, T. Wang, W. Zhang, L. Li, X. Lv and H. Wang, *Dalton Transactions*, 2024, **53**, 5534-5543.
6. Y. Song, W. Zhan, Z. Wu, Q. Chen, X. Chen, Z. Liu, J. Du, C. Tao and Q. Zhang, *Journal of Materials Chemistry A*, 2024, **12**, 16910-16920.
7. F. Tang, J. Gao, Q. Ruan, X. Wu, X. Wu, T. Zhang, Z. Liu, Y. Xiang, Z. He and X. Wu, *Electrochimica Acta*, 2020, **353**, 136570.
8. L. Cao, Z. Gao, G. Lu, X. Chen, Y. Li, Y. Wu, R. Wang, H. Yuan, J. Hu, F. Wei, Z. Ji, Y. Sui, Q. Meng, L. Li and L. Zhang, *Colloids and Surfaces A: Physicochemical and Engineering Aspects*, 2023, **676**, 132295.
9. S. Li, Y. Wei, Q. Wu, Y. Han, G. Qain, J. Liu and C. Yang, *Materials Letters*, 2023, **348**.
10. Q. Xie, G. Cheng, T. Xue, L. Huang, S. Chen, Y. Sun, M. Sun, H. Wang and L. Yu, *Materials Today Energy*, 2022, **24**, 100934.
11. Y. Liu, Y. Wang, X. Zhang, Y. Song, Y. Yi, H. Yin, Y. Zhu, G. Xu and Y. Zheng, *ACS Materials Letters*, 2023, **5**, 2820-2828.
12. S.-C. Ma, M. Sun, S.-X. Wang, D.-S. Li, W.-L. Liu, M.-M. Ren, F.-G. Kong, S.-J. Wang and Y.-M. Xia, *Scripta Materialia*, 2021, **194**, 113707.
13. H. Yu, J. Sun, Z. Wang, M. Ren, Z. Yang, W. Liu, J. Yao, C. Zhang and H. Zhao, *Journal of Sol-Gel Science and Technology*, 2023, DOI: 10.1007/s10971-023-06201-y.
14. L. Qin, Q. Zhu, L. Li, H. Cheng, W. Li, Z. Fang, M. Mo and S. Chen, *Journal of Solid State Electrochemistry*, 2023, **27**, 773-784.
15. B. Yang, D. Li, S. Wang, C. Sun and N. Wang, *ACS Applied Materials & Interfaces*, 2022, **14**, 18476-18485.
16. Q. Zi-Wei, *Chinese Journal of Structural Chemistry*, 2021, **40**, 1535–1540.
17. C. Li, C. Zheng, H. Jiang, S. Bai and J. Jia, *Journal of Alloys and Compounds*, 2021, **882**, 160587.
18. X. Wu, S. Zhou, Y. Li, S. Yang, Y. Xiang, J. Jiang, Z. Liu, D. Fan, H. Zhang and L. Zhu, *Journal of Alloys and Compounds*, 2021, **858**, 157744.